Astron. Astrophys. 318, L17–L20 (1997)

ASTRONOMY AND ASTROPHYSICS

LETTER

Letter to the Editor

Influence of non-thermal processes on line asymmetries in solar flares

M.D. Ding[1,2] **and C. Fang**[2]

[1] Kiepenheuer-Institut für Sonnenphysik, Schöneckstr. 6, D-79104 Freiburg, Germany
[2] Department of Astronomy, Nanjing University, Nanjing 210093, China

Received 3 September 1996 / Accepted 28 November 1996

Abstract. We make line profile calculations for a flare atmosphere considering simultaneously the effect of non-thermal excitation and ionization of the hydrogen atoms caused by precipitating high-energy electrons, and the effect of possible chromospheric downflows. The results confirm the earlier finding that a downflow, if confined to the upper chromosphere, can sometimes produce a blue asymmetry of the Hα line. In addition, we find that the existence of such non-thermal effects tends to enhance the blue-asymmetry magnitude. In particular, the larger the energy flux, or the harder the energy spectrum for the beam electrons, the easier it will be to produce a blue-asymmetric Hα profile, which is simultaneously intensified and broadened. Possible reasons which make the blue asymmetry less popular than the red asymmetry in observations are discussed.

Key words: Line: profiles – Sun: flares

1. Introduction

The asymmetry of chromospheric lines in solar flares has been discovered long ago, but it remains to be a puzzling problem. Most frequently, a red asymmetry is observed during the flare impulsive phase. Usually, such a red asymmetry is interpreted as the result of chromospheric downflows (e.g., Ichimoto & Kurokawa 1984; Wülser & Marti 1989; de la Beaujardière et al. 1992), which are believed to be virtually a downward-propagating chromospheric condensation. Numerical simulations of gas dynamics in the flare loop, when imposed to an impulsive energy deposition, show that the chromospheric condensation is driven by the over-heating in the transition region which, in the mean time, gives rise to the upward chromospheric evaporation (Fisher et al. 1985; Gan et al. 1991).

Send offprint requests to: M.D. Ding (Nanjing University)

On the other hand, many evidences showing the existence of a blue asymmetry for chromospheric lines of flares have appeared (Heinzel et al. 1994). The problem is more complicated when blue and red asymmetries are observed simultaneously at different positions in a flaring region (Canfield et al. 1990), or at a same position but different times (Ji et al. 1994). Canfield et al. (1990) have interpreted the blue asymmetry as being caused by an upward motion in the middle chromosphere due to a local pressure excess or some MHD processes. While such possibilities cannot be ruled out, recent line profile calculations show that a downward motion, when confined to the lower transition region or upper chromosphere, can also produce the blue asymmetry of line profiles, under some special circumstances (see e.g., Gan et al. 1993; Heinzel et al. 1994). The physical essence is that when the flare atmosphere is not strongly disturbed (i.e., the coronal mass density and the chromospheric temperature are not too high), the line source function in the upper chromosphere shows a sharp decrease towards upper layers and the effect of a downward motion there is to cause a red-wing absorption. The fact that the observed blue asymmetry more probably exists in those centrally reversed line profiles (Švestka 1976) seems to favor such an explanation.

Recently, Fang et al. (1993) studied the flare Hα and Ca II K lines with the inclusion of non-thermal excitation and ionization effect of hydrogen and calcium atoms caused by the bombardment of precipitating high-energy electrons, which are considered to be the main flare heating source. Their results show that the non-thermal effect plays an important role in determining the line intensity and width, especially for Hα. In order to have a clearer knowledge in line profile diagnostics for solar flares, we need to study in more detail how such a non-thermal effect influences the line asymmetries. In this paper we perform systematic calculations for the Hα line profile when both the non-thermal effect and the velocity field are considered, and then check how the line asymmetry varies in response to these factors.

2. Numerical Method

2.1. General Procedure

A fully consistent and accurate treatment of the flare hydrodynamics together with its radiative transfer is extremely difficult and has not yet been achieved. Canfield & Gayley (1987) computed the Hα emission from dynamic atmospheres by use of the probabilistic radiative transfer method. As the authors indicated, such a method loses accuracy in the presence of large velocity gradients. The present work, however, will not treat the flare dynamics in detail but use a better code of the radiative transfer.

We employ the same program as that used by Fang et al. (1993) to compute the line profiles from an atmosphere with a prescribed temperature versus column mass density relation and a velocity field. The program solves the equations of statistical equilibrium and radiative transfer iteratively until a convergence is reached. A four-level-plus-continuum atomic model for hydrogen is adopted here. The line broadening mechanisms include the Doppler effect, Stark effect, radiative damping, and resonance broadening.

In particular, the non-thermal excitation and ionization transition rates caused by a possible precipitating electron beam have been included in the statistical equations, i.e., these rates are added to the radiative and thermal collisional rates which are normally considered. To do so, we first calculate the energy deposit rates at different atmospheric layers by an electron beam with given flux and power index values. The non-thermal transition rates are then evaluated according to their relative collisional cross-sections. All formulae related to this problem can be found in Fang et al. (1993).

2.2. Description of the Velocity Field

The existence of a velocity field makes the local atomic absorption (emission) profile Doppler shifted, thus changing the radiative transition rates and ultimately the line source function. In some special cases when the non-thermal collisional transition rates dominate over the radiative rates, the statistical equilibrium will keep relatively stable against the variation of the velocity field. Thus the effect of the velocity field is mainly concentrated on producing an asymmetric line profile, whose asymmetry property depends on whether the moving layer is absorptive or emissive relative to the underlying intensity irradiated on it (Ding & Fang 1996).

Supposing that the chromospheric mass motion is caused by the downward propagation of a condensation, the moving region should be located lower and lower with time elapsing. Numerical simulations of the gas dynamics in the flare loop show that the condensation is restricted in a very narrow region when it is primarily formed (e.g., Fisher et al. 1985) and is expected to expand somewhat during its downward propagation and dissipation. To simplify this problem, we will consider in the following only the case of an atmosphere purely superimposed by an arbitrary velocity field, which is assumed to be confined to different heights but occupy a small vertical space (i.e., only 2–3 grid points of the atmosphere have a non-zero velocity value). Of course, such simple kinetic descriptions represent no real situations of flare dynamics and the following results can only be taken as suggestive.

3. Results and Discussions

3.1. Non-thermal Effect on Line Asymmetries

Ding & Fang (1996) have shown that a downward velocity field can be responsible for both the blue asymmetry and the red asymmetry of the Hα line, provided that the velocity field is confined to different heights in the upper chromosphere. The Ca II K line, however, mostly shows a red asymmetry. Here we study in more detail the influence of various electron beams on the asymmetry property of the Hα line.

We adopt five atmospheric models with a same temperature structure (F1 model of Machado et al. 1980), but different moving regions, which are located at heights of H = 1356, 1318, 1279, 1241, and 1202 km, with nearly the same widths of about 23 km. (The height at the top chromosphere in the F1 model is $\sim$ 1428 km). The velocity value is assumed to be 30 km s^{-1} and uniform within the moving region. For the electron beam, we assume that the electrons have a power law energy distribution and a low cut-off energy of E_1 = 20 keV. Five energy fluxes $\mathscr{F}_1$ = 10^{10}, 3 10^{10}, 10^{11}, 3 10^{11}, and 10^{12} ergs cm^{-2} s^{-1} with power indices δ = 3, 4, and 5 are considered. Figure 1 displays the Hα line profiles calculated at the disk center for all the above circumstances. A Gaussian macro-turbulent velocity of 20 km s^{-1} has been used to convolve these profiles.

Figure 1 reveals some interesting phenomena. First, as has already been pointed out by Fang et al. (1993), the non-thermal effect of electron beams causes the Hα line profile to be more intensified and broadened, compared to the case without including the non-thermal effect. Second, downward mass motions can make the profile either blue-asymmetric or red-asymmetric, depending on the vertical location of the velocity field (Ding & Fang 1996). In addition to these, we can notice another fact that, the line asymmetry also depends on the parameters of the electron beam: an intense (large $\mathscr{F}_1$) or hard (small δ) beam makes the profile more probable to have a blue asymmetry. In other words, many examples can be found that for the same distribution of temperature and velocity field (i.e., the same column in Fig. 1), the generated profile can vary from red-asymmetric to blue-asymmetric as $\mathscr{F}_1$ increases or δ decreases.

3.2. A Brief Interpretation

The reason for the above results is the following: the height distribution of the line source function depends sensitively on the parameters of $\mathscr{F}_1$ and δ of the electron beams (see Hénoux et al. 1993), and one can anticipate that the same moving region may have different absorption (emission) properties relative to

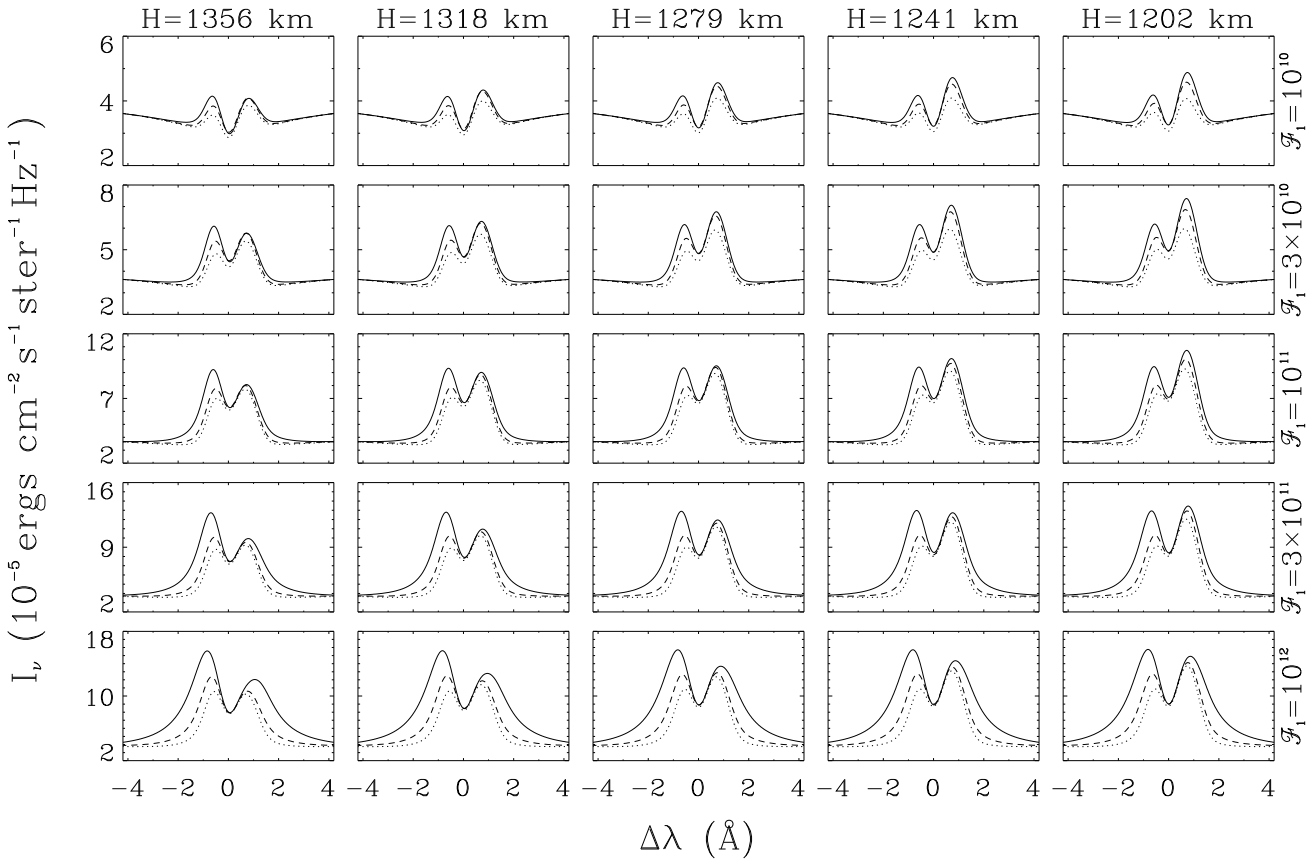

Fig. 1. Asymmetric Hα line profiles computed from the F1 model with five moving regions confined to different atmospheric heights (from left to right in each row), and with the non-thermal effect of electron beams with five fluxes (from top to bottom in each column). The fluxes are in units of ergs cm^{-2} s^{-1}. Different cases for power indices are indicated by line types (δ = 3: solid lines; δ = 4: dashed lines; δ = 5: dotted lines). Notice the different intensity scales for different rows

the underlying specific intensity in different $\mathscr{F}_1$ and δ cases. To show this point clearly, we plot in Fig. 2 the Hα line source functions (S_ν) with a fixed $\mathscr{F}_1$ but various δ values, and a fixed δ but various $\mathscr{F}_1$ values. The velocity region is confined to the height of 1356 km, which can be distinguished by a slight dip in the S_ν curves. Also plotted in the figure are the heights of optical depth unity at $\Delta\lambda$ = 1.0, 2.0, and 3.0 Å.

Figure 2a shows that the effect of decreasing δ is mainly to raise the source function in the middle chromosphere, while the line-formation height is not changed significantly, due to the large opacity in the red wing produced by the moving region. These two factors help to produce a more intense wing emission. Correspondingly, the moving region in the upper chromosphere will absorb more photons in the red wing and make the emergent profile less red-asymmetric or more blue-asymmetric. For the case of increasing $\mathscr{F}_1$, the source function is enhanced as well but in a slightly different way. However, the effect on the line asymmetries can be expected to be similar.

Although we have obtained many examples of Hα line profiles with blue asymmetry (see Fig. 1), this does not imply there is a large probability in detecting the blue asymmetry in observations. First, one should be aware that the production of blue-asymmetric profile needs some special conditions including the existence of an intense and hard electron beam, and a moving region confined to higher layers. Such a circumstance can only appear in the early impulsive phase and at the foot point where the electron beam bombardment occurs. Thus it is a very short-lived and spatially restricted phenomenon. Another fact comes from our simplification in the flare dynamics. A real flare is much more complex, involving differentially distributed and rapidly changing velocity fields, as well as other atmospheric parameters, which can smooth out the source function distribution to some extent and reduce the appearance of blue asymmetry. These reasons account for why blue asymmetries are less popular than red asymmetries in flare spectral observations.

4. Conclusions

We have performed line profile calculations for a flare atmosphere including the effect of non-thermal excitation and ionization of the hydrogen atoms caused by precipitating high-energy

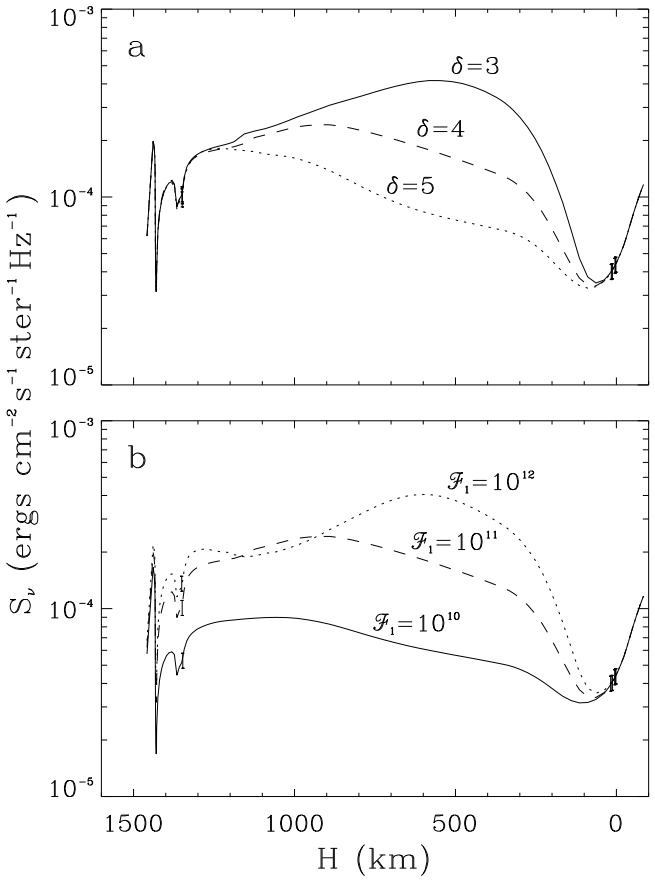

Fig. 2. Hα line source functions computed from the F1 model with non-thermal effects included for **a** $\mathscr{F}_1$ = 10^{11} ergs cm^{-2} s^{-1} while δ = 3, 4, and 5, and **b** δ = 4 while $\mathscr{F}_1$ = 10^{10}, 10^{11}, and 10^{12} ergs cm^{-2} s^{-1}. From left to right, the three short vertical bars on each curve represent heights of optical depth unity at $\Delta\lambda$ = 1.0, 2.0, and 3.0 Å, respectively

electrons, and the effect of possible chromospheric downflows. The results confirm the earlier finding that a downflow, if confined to the upper chromosphere, can sometimes produce a blue asymmetry of the Hα line. In addition, we find that the existence of such non-thermal effects tends to enhance the blue-asymmetry magnitude. In particular, the larger the energy flux, or the harder the energy spectrum for the beam electrons, the easier it will be to produce a blue-asymmetric Hα profile, which is simultaneously intensified and broadened. As we have made some simplifications in our model, further computations which can treat the radiative transfer and gas dynamics in detail are needed to check these results.

It should also be noted that the computations are model-dependent. However, we find that the general conclusions above are valid for a wide variety of model atmospheres. Besides the temperature structure and the velocity field, other important parameters include the column mass density of the corona (m_c) and that at the source of high-energy electrons (m_e). For the latter, a more appropriate parameter is $m_c - m_e$, i.e., the column mass that non-thermal electrons have to penetrate before reaching the chromosphere. In this work, we have adopted m_c = 3.14 10^{-4} g cm^{-2} given by the F1 model and m_e = 0, assuming that the electron source is located far above the transition region.

If we set a lower located source site of high-energy electrons (smaller $m_c - m_e$), the non-thermal excitation and ionization effect will become more obvious, especially in the upper chromosphere. Therefore, this can lead to a relative increase of the line source function there. In most cases, it makes the computed line profile slightly less possible to show a blue asymmetry, if other parameters remain unchanged. On the other hand, a higher coronal mass density (larger m_c) tends to enhance the thermal collisional transition rates in the upper chromosphere. Its effect on the line asymmetries will depend on the relative importances of thermal and non-thermal collisional rates.

Acknowledgements. One of the authors (M.D.D.) would like to thank the staff of the Kiepenheuer-Institut for their kind hospitality during his visit there. Critical comments from the referees are highly appreciated. Thanks are also due to Dr. H. Balthasar for a careful reading of the manuscript and making some suggestions.

References

Canfield R.C., Gayley K.G., 1987, ApJ 322, 999
Canfield R.C., Kiplinger A.L., Penn M.J., Wülser J.P., 1990, ApJ 363, 318
de la Beaujardière J.-F., Kiplinger A.L., Canfield R.C., 1992, ApJ 401, 761
Ding M.D., Fang C., 1996, Solar Phys. 166, 437
Fang C., Hénoux J.C., Gan W.Q., 1993, A&A 274, 917
Fisher G.H., Canfield R.C., McClymont A.N., 1985, ApJ 289, 414
Gan W.Q., Fang C., Zhang H.Q., 1991, A&A 241, 618
Gan W.Q., Rieger E., Fang C., 1993, ApJ 416, 886
Heinzel P., Karlický M., Kotrč P., Švestka Z., 1994, Solar Phys. 152, 393
Hénoux J.C., Fang C., Gan W.Q., 1993, A&A 274, 923
Ichimoto K., Kurokawa H., 1984, Solar Phys. 93, 105
Ji G.P., Kurokawa H., Fang C., Huang Y.R., 1994, Solar Phys. 149, 195
Machado M.E., Avrett E.H., Vernazza J.E., Noyes R.W., 1980, ApJ 242, 336
Švestka Z., 1976, Solar Flares, Reidel, Dordrecht
Wülser J.-P., Marti H., 1989, ApJ 341, 1088

This article was processed by the author using Springer-Verlag LaTeX A&A style file *L-AA* version 3.